Causal influences of El Niño–Southern Oscillation on global dust activities

Thanh Le[1⋆] and Deg-Hyo Bae[1⋆]

[1]Department of Civil and Environmental Engineering, Sejong University, Seoul 05006, Republic of Korea

⋆*Correspondence to*: Deg-Hyo Bae (dhbae@sejong.ac.kr) and Thanh Le (levinhthanh.lvt@gmail.com)

Abstract. The dust cycle is an important element of the earth system and further understanding of the main drivers of dust emission, transport and deposition is necessary. The El Niño–Southern Oscillation (ENSO) is the main source of interannual climate variability and is likely to influence the dust cycle on a global scale. However, the causal influences of ENSO on dust activities across the globe remain unclear. Here we investigate the response of dust activities to ENSO using output from Coupled Modeling Intercomparison Project Phase 6 (CMIP6) historical simulations during the 1850-2014 period. The analyses consider the confounding impacts of the Southern Annular Mode, the Indian Ocean Dipole, and the North Atlantic Oscillation. Our results show that ENSO is an important driver of dry and wet dust deposition over the Pacific, Indian, Southern, and parts of Atlantic Oceans during 1850-2014. Over continents, ENSO signature is found in America, Australia, parts of Asia, and Africa. Further, ENSO displays significant impacts on dust aerosol optical depth over oceans, implying the controls of ENSO on the transport of atmospheric dust. Nevertheless, the results indicate that ENSO is unlikely to exhibit causal impacts on regional dust emissions of major dust sources. While we find high consensus across CMIP6 models in simulating the impacts of ENSO on dust deposition and transport, there is little agreement between models for the ENSO causal impacts on dust emission. Overall, the results emphasize the important role of ENSO in global dust activities.

Keywords: El Niño–Southern Oscillation; dust transport; causal signatures; dust deposition; dust emission; CMIP6.

1 Introduction

The dust cycle is an important component of the earth system (Bullard et al., 2016; Carslaw et al., 2010; Jickells et al., 2005; Knippertz and Todd, 2012). Dust may alter the balance of the radiative forcing of the climate system (Carslaw et al., 2010; Schulz et al., 2012; Xu et al., 2017), and changes in dust transport and distribution may have impacts on regional climate (Creamean et al., 2013; Evan et al., 2011; Kok et al., 2018; Li et al., 2019; Rotstayn et al., 2011; Scott et al., 2018; Yang et al., 2017). Dust deposition is a source of nutrients (e.g., dust iron, phosphorus, and nitrogen) for land and ocean ecosystems (Bao et al., 2017; Fan et al., 2006; Jickells et al., 2005; Jiménez et al., 2018; Kanakidou et al., 2018; Schulz et al., 2012; Tagliabue et al., 2010). In particular, long-range transport of mineral dust may alter the global biogeochemical cycles and regional soil composition (D'Odorico et al., 2013; Duan et al., 2021; Perry et al., 1997; Prospero and Mayol-Bracero, 2013). On the other hand, dust transports may cause pollution and have significant impacts on human health (Li et al., 2021; de

Longueville et al., 2013; Shahsavani et al., 2020; Tong et al., 2017; Yang et al., 2017) and environments (Guo et al., 2017; Li et al., 2019; Perry et al., 1997; Xu et al., 2017; Zhang et al., 2018).

Dust emission, transport, and deposition are driven by vegetation cover, soil moisture, precipitation, and wind speed (Carslaw et al., 2010; Kanakidou et al., 2018; Kok et al., 2021; Pi et al., 2019; Thornhill et al., 2020). Hence, ENSO impacts on these variables (Cai et al., 2021; Le et al., 2022; Le and Bae, 2020; Yeh et al., 2018) are likely to result in ENSO-induced changes in dust activities. For instance, ENSO is shown to have influences on dust activities over Australia (Marx et al., 2009), the Sahara and Amazon basin (Boy and Wilcke, 2008), the regions from the Arabian Peninsula to Central Asia (Huang et al., 2021), South America (Shao et al., 2013), and East Asia (Jeong et al., 2018). Nevertheless, ENSO influences on the dust cycle remain elusive. In particular, little effort has been made to evaluate the causal effects of ENSO on dust activities on a global scale.

While there are limited observational records of past dust deposition over oceans (van der Does et al., 2020), Earth system models contribute crucial data sets to examine the influences of ENSO on global dust activities. Recently, there is improvement in understanding the global dust cycle (Kok et al., 2021) and simulating dust aerosol in Earth system models (Collins et al., 2017; Mulcahy et al., 2020; Thornhill et al., 2020; Zhao et al., 2022). Particularly, Coupled Modeling Intercomparison Project Phase 6 (CMIP6) models (Eyring et al., 2016) are provided with better description of the aerosol model and the atmospheric chemistry model and allow for a clearer understanding of ENSO impacts on dust activities.

In this work, we investigate the causal effects of ENSO on global dust activities. We consider the confounding influences of other main climate modes (i.e., the Indian Ocean Dipole (IOD), the Southern Annular Mode (SAM), and the North Atlantic Oscillation (NAO)). Further understanding of the linkages between ENSO and dust cycles at a global scale may contribute to the predictions of future dust events and their impacts under a changing environment.

2 Data and methods

2.1 Datasets

We employed monthly data of the following variables: dry deposition rate of dust (i.e., dry deposition due to gravitational settling, impacts scavenging and turbulent deposition; dry dust), wet deposition rate of dust (i.e., the surface deposition rate of dust due to wet processes; wet dust), dust optical thickness at 550nm (i.e., total atmospheric aerosol optical depth due to dust at a wavelength of 550 nanometers; od550dust) and emission rate of dust (emidust). Dry dust and wet dust are important variables of dust deposition flux at land and ocean surface (Schulz et al., 2012), while od550dust represents the properties, transport, and distribution of dust in the atmosphere (Bullard et al., 2016; Collins et al., 2017). Dust emission is dependent on wind speed (or wind stress), land vegetation (e.g., leaf area index), and soil moisture (or soil type) (Kok et al., 2021). We used monthly sea surface temperature (SST) and sea level pressure (SLP) to calculate the time series of the main modes of climate variability (see also section 2.2 Methods and section Text S1). These datasets were taken from the historical experiment (Eyring et al., 2016) covering the period 1850-2014. Tables S1 and S2 list the 12 CMIP6 models (with accessible

dust-related data) utilized in the present work. We limited our study to all the models having both dry dust and wet dust data (i.e., there is total of 12 models with accessible dry dust and wet dust data as described in Table S2). Dust deposition on land and ocean surface are important metrics to assess the impacts of dust activities on ecosystems and environment (Bao et al., 2017; Fan et al., 2006; Jickells et al., 2005; Jiménez et al., 2018; Kanakidou et al., 2018; Schulz et al., 2012). Additional data of od550dust and emidust supplied by these 12 models provide further understanding of ENSO impacts on dust activities.

2.2 Methods

Following the methodology utilized in recent works (Le et al., 2021; Le and Bae, 2020), we evaluate the null hypothesis of no Granger causality between ENSO and dust activities (i.e., dust deposition rate, dust optical thickness, and emission rate of dust) by using a multivariate predictive model (see Text S1). We use the following multivariate predictive model (Mosedale et al., 2006; Stern and Kaufmann, 2013) to estimate the causal links between the ENSO and dust deposition:

$$\boldsymbol{X_t} = \sum_{i=1}^{p} \boldsymbol{\alpha_i X_{t-i}} + \sum_{i=1}^{p} \boldsymbol{\beta_i Y_{t-i}} + \sum_{j=1}^{m} \sum_{i=1}^{p} \boldsymbol{\delta_{j,i} Z_{j,t-i}} + \boldsymbol{\varepsilon_t} \quad (1)$$

where X_t is the annual mean (or seasonal mean) dust deposition for year t, Y_t is the ENSO index, and $Z_{j,t}$ is the confounding factor j for year t. In the predictive model presented in equation 1, while assessing the effect of Y on X (i.e., the contribution of the term $\sum_{i=1}^{p} \beta_i Y_{t-i}$ in predicting X), the possible influence of past X events are considered by adding the term $\sum_{i=1}^{p} \alpha_i X_{t-i}$. Thus, the causal influence of Y on X, if detected, is robust and the impact of past X events are accounted in the analyses. Here, m is the number of confounding factors and $p \geq 1$ is the order of the multivariate predictive model. The optimal order p is computed by minimizing the Schwarz criterion or the Bayesian information criterion (Schwarz, 1978). The optimal orders may be different for each model.

Here we take into account the impacts of confounding factors and therefore provide further information of the real-world teleconnections. In the analyses, we use three different confounding factors; hence, m is equal to 3. The noise residuals ε_t and the regression coefficients α_i, β_i and $\delta_{j,i}$ are computed by using the multiple linear regression analysis of the least squares method. We detrend and normalize all the climate indices.

In the analyses, we investigated the confounding effects of other main climate modes (i.e., the SAM (e.g., Cai et al., 2011), the IOD (Saji et al., 1999; Webster et al., 1999), and the NAO (Hurrell et al., 2003)) on the links of ENSO and dust activities. The climate modes SAM, the IOD and the NAO are the important sources of global climate variability (Hurrell et al., 2003; Luo et al., 2012; Roxy et al., 2015). For instance, the NAO is the prominent mode of atmospheric circulation variability over the North Atlantic and surrounding regions (Delworth et al., 2016; Hurrell et al., 2003) and variations in NAO are crucial for the environment and society (Hurrell et al., 2003). The IOD affects climate extremes over the Indian Ocean and surrounding areas (Abram et al., 2008; Kripalani et al., 2009; Kripalani and Kulkarni, 1997) and might cause severe economic consequences (Ummenhofer et al., 2009). The SAM is the major mode of atmospheric circulation variability in the southern Hemisphere (Cai et al., 2011; Raphael and Holland, 2006). In addition, changes in these modes may affect the variations of ENSO (Abram et al., 2020; Cai et al., 2011, 2019; Le et al., 2020; Le and Bae, 2019).

Nevertheless, it is likely that these factors may alter the influences of ENSO on dust activities. Further information on the methods is explained in Text S1.

3 Results

3.1 ENSO impacts on dust deposition, transport, and emission

Figure 1 denotes the causal influences of ENSO on the annual mean deposition rate of dry dust (a) and west dust (b) over the 1850-2014 period of the historical experiment. The results in Figure 1 are described as the ensemble mean of 12 models (see Tables S1 and S2). We show that ENSO plays an important role in dust deposition over the Pacific, Indian, Southern Oceans, parts of Atlantic Oceans, and the surrounding continents. In particular, ENSO exhibits a signature on both dry and wet dust deposition processes over the subarctic North Pacific, parts of the southern Arctic Ocean, and Antarctica. In these areas, the *p*-value is lower than 0.33 (and 0.1), suggesting that ENSO is unlikely (and very unlikely) to exhibit no causal effects on dust deposition.

Further analyses reveal that ENSO displays significant impacts on aerosol optical depth over Oceans, implying the controls of ENSO on the transport of atmospheric dust (Figure 2a). Figure 2b shows the scale of ENSO causal impacts on global dust activities. In Figure 2b, the areas influenced by ENSO are computed as the areas limited by the cyan contour line as shown in Figures 1 and 2a (i.e., *p*-value is lower than 0.33 or ENSO is unlikely to exhibit no causal effects on dust activities over these regions). Over oceans, the areas affected by ENSO are estimated at approximately 17.6%, 32.3%, and 20.7% of total earth surface (i.e., 24.9%, 45.6% and 29.2% of total ocean areas) for deposition of dry dust, dust aerosol optical depth, and deposition of wet dust, respectively (Figure 2b). The land areas affected by ENSO are estimated at approximately 5.1%, 7.5%, and 6.8% of the total earth surface (i.e., 17.5%, 25.7% and 23.3% of total land areas) for deposition of dry dust, dust aerosol optical depth, and deposition of wet dust, respectively (Figure 2b).

The causal effects of ENSO on seasonal mean dry dust deposition are shown in Figure S1. The largest impacts of winter (DJF) ENSO are observed in the following spring (MAM), with approximately 3.4% of total earth surface over land (i.e., 11.6% of total land areas) and approximately 16% of total earth surface over the ocean (i.e., 22.6% of total ocean areas) are affected (Figure S2). The impacts of ENSO on dry dust deposition gradually decrease in the following summer, fall, and winter (Figures S1 and S2). In particular, the influences of ENSO on winter dry dust deposition are mainly limited in Antarctica (approximately 0.5% of total earth surface or 1.7% of total land areas) and the tropical Pacific (approximately 0.7% of total earth surface or 1% of total ocean areas).

The results in Figure 3 demonstrate that ENSO is less likely (i.e., *p*-value > 0.33) to exhibit causal impacts on regional dust emissions of major dust sources (e.g., over Northern Africa, the Middle East, and central Asia).

3.2 Models' consensus of ENSO effects on dust activities

High consensus across models is noted for the large causal effects of ENSO on global dust deposition (Figure 1) and transport (Figure 2a). However, there is little consensus across models for the impacts of ENSO on dust emissions (i.e., a limited area in central Australia, Figure 3).

Figure 4 shows the findings of 12 different models (see Tables S1 and S2) for the causal effects of ENSO on dry dust over the 1850-2014 period of the historical experiment. The results for wet dust are shown in Figure S3. The response of dry dust deposition is underestimated in the models CanESM5, CNRM_ESM2_1, and INM-CM4-8 compared to the models mean (Figure 1a). Over Europe and northern Africa, the model MIROC-ES2L exhibits a clearer response of dry dust deposition to ENSO compared to other models. Most models suggest a strong response of dry dust deposition to ENSO over the tropical Pacific.

Figure 5 shows the results of 9 individual models (see Table S2) for the causal influences of ENSO on dust aerosol optical depth over the 1850-2014 period. Consistent with Figure 4, the response of dust aerosol optical depth to ENSO is weaker in the models CanESM5 and INM-CM4-8 compared to others. The results described in Figures 4 and 5 indicate that the models agree well on the causal signatures of ENSO on the spatiotemporal evolution of dust.

Figure 6 shows the response of dust emissions to ENSO in 11 different models (see Table S2). ENSO may initiate dust activities in limited regions over Australia (CESM2, CESM2_WACCM, INM-CM4-8, INM-CM5-0, MIROC6 and UKESM1_0_LL), southern Africa (CESM2, CESM2_WACCM, INM-CM4-8, MIROC6 and UKESM1_0_LL), southern South America (UKESM1_0_LL), and southwestern North America (INM-CM4-8, INM-CM5-0, and UKESM1_0_LL). Several models (i.e., INM-CM5-0, UKESM1_0_LL) exhibit stronger ENSO signals on dust emissions compared to other models. The response of dust emissions to ENSO is much less apparent in the models CESM2_FV2 and CESM2_WACCM_FV2. As most models do not include high-latitude dust sources (Kok et al., 2021), the impacts of ENSO on dust emissions of high-latitude are not visible.

4 Discussion

Based on the trace of dust deposition as shown in Figure 1, ENSO-induced dust deposition in the North Pacific is likely originated from major dust sources regions over central and eastern Asia, consistent with previous work (Jickells et al., 2005). Dust deposited in the tropical Pacific might come from multiple dust sources over Australia, southwestern North America, or even South America. Figure 1 suggests that dust supply to the South Indian Ocean might be originated from a small dust source over South Africa, while dust deposition over the tropical Atlantic is associated with a major dust source of West Africa, potentially contributing to variations of the Atlantic Meridional Mode (Evan et al., 2011). As dust particles might be carried by winds between different regions (Guo et al., 2017; Yang et al., 2017), the influences of ENSO on global atmospheric circulation and rainfall (Yeh et al., 2018) lead to ENSO-induced changes in spatial pattern of dust deposition. For example, ENSO impacts on winds and precipitation over the tropical Pacific (Dai and Wigley, 2000; Le and Bae, 2020)

contribute to the causal effects of ENSO on dry and wet dust deposition over this region (Figure 1). In addition, ENSO atmospheric teleconnections over Australia, North and South Americas (Ashok et al., 2007; Garfinkel et al., 2013; Taschetto and England, 2009; Yu and Zou, 2013) play an important role on dust deposition in these regions (Figure 1).

Significant impacts of ENSO on atmospheric aerosol loading (Figures 2a and 5) may lead to a strong response of marine productivity (i.e., the production of organic matter in the ocean from carbon dioxide by phytoplankton) to ENSO. For example, there is strong correlation between aerosol optical depth and iron deposition and satellite chlorophyll (Carslaw et al., 2010; Jickells et al., 2005). The controls of ENSO on the transport of atmospheric dust (Figure 2a) are consistent with the influences of ENSO on global wind patterns (Dai and Wigley, 2000; Le and Bae, 2020; Yeh et al., 2018). As dust deposition over the ocean and lakes may provide important nutrients for phytoplankton development, productivity, and carbon uptake (Jickells et al., 2005; Jiménez et al., 2018), ENSO may potentially modulate oceanic biogeochemistry and the carbon cycle over Pacific, Indian and Southern Oceans. For example, expansions in the dust supply of iron to the ocean may result in a decrease in atmospheric CO_2 (Kohfeld et al., 2005). The phytoplankton growth productivity (Tagliabue et al., 2010) of the Southern Ocean strongly relies on the dust deposition from major dust sources, thus, ENSO may indirectly influence the marine productivity and atmospheric CO_2 level.

The causal impacts of ENSO on dust deposition over South America (Figure 1) are consistent with previous studies (Boy and Wilcke, 2008; Shao et al., 2013). Figures 1 and 2 show an agreement with recent works for the potential influences of ENSO on dust activities over regions from Arabian Peninsula to Central Asia (Huang et al., 2021) and East Asia (Jeong et al., 2018). Substantial influences of ENSO on dust emission over central Australia (Figure 3) suggest an agreement with earlier work (Marx et al., 2009), while we observe weak causal impacts of ENSO on regional dust emissions of major dust sources (Figure 3). As the consistency between models is low (Figure 3), large uncertainties remain for the causal impacts of ENSO on dust emissions. Previous studies indicate the important role of human influences in igniting local dust activities (Duniway et al., 2019; Webb and Pierre, 2018). For example, as anthropogenic land management leads to changes in land surface properties and dust availability (Jickells et al., 2005), an increase in population is likely to intensify dust emission and long-range dust transport (Moulin and Chiapello, 2006). Hence, the impacts of human activities and changes in land use on regional dust emissions might be a topic of future works.

Regarding the consistency across models, the response of dust emission to ENSO is much stronger in the models INM-CM5-0, MIROC-ES2L, and UKESM1_0_LL compared to other models (Figure 6). This difference might be due to the use of different dust schemes and soil properties in this model which lead to higher dust emissions (Mulcahy et al., 2020; Zhao et al., 2022). As models use different parameters to estimate dust emissions (Thornhill et al., 2020), this discrepancy leads to low consensus across models in modeling the response of dust emissions to ENSO (Figures 3 and 6).

5 Conclusions

In this study, we showed that ENSO exhibits significant causal impacts on global dust deposition and transport (Figures 1, 2, 4, and 5). However, we observed large uncertainty in the causal signatures of ENSO on regional dust emissions of major dust sources (Figures 3 and 6).

As high-resolution models may improve the simulations of dust emission processes (Knippertz and Todd, 2012) and their connection with ENSO, further studies might use outputs from high-resolution models. Because there is a strong link between dust deposition over ocean and ocean biogeochemistry and carbon cycle (Rap et al., 2018) and there are possible changes in ENSO properties under a warming environment (Cai et al., 2021; Timmermann et al., 2018; Yeh et al., 2018), further works related to ENSO impacts on oceanic carbon cycle are necessary. While there is uncertainty in the projections of global dust deposition (Carslaw et al., 2010) and there is low confidence in projecting dust activities under greenhouse warming (Thornhill et al., 2020), additional studies may focus on the future impacts of ENSO on dust activities.

Data availability

CMIP6 data can be accessed from the ESGF website at https://esgf-node.llnl.gov/search/cmip6/.

Author contribution

TL designed the study, performed the data analysis, and wrote the manuscript. DHB contributed to the interpretation of results and the writing of the manuscript.

Competing interests

The authors declare that they have no conflict of interest.

Financial support

This work is supported by the National Research Foundation of Korea (NRF) grant funded by the Korea government (MSIT) (Grant No. 2021R1G1A1004389).

Acknowledgments

The authors thank the anonymous reviewers for their valuable comments and suggestions. We acknowledge the World Climate Research Programme, which through its Working Group on Coupled Modelling, coordinated and promoted CMIP6. We thank the climate modelling groups (listed in Table S1) for producing and making available their model output, the Earth

System Grid Federation (ESGF) for archiving the data and providing access, and the multiple funding agencies who support CMIP6 and ESGF. CMIP6 data can be accessed from the ESGF website at https://esgf-node.llnl.gov/search/cmip6/. T Le is supported by the National Research Foundation of Korea (NRF) grant funded by the Korea government (MSIT) (Grant No. 2021R1G1A1004389).

References

Abram, N. J., Gagan, M. K., Cole, J. E., Hantoro, W. S. and Mudelsee, M.: Recent intensification of tropical climate variability in the Indian Ocean, Nat. Geosci., 1(12), 849–853, doi:10.1038/ngeo357, 2008.

Abram, N. J., Wright, N. M., Ellis, B., Dixon, B. C., Wurtzel, J. B., England, M. H., Ummenhofer, C. C., Philibosian, B., Cahyarini, S. Y., Yu, T.-L., Shen, C.-C., Cheng, H., Edwards, R. L. and Heslop, D.: Coupling of Indo-Pacific climate variability over the last millennium, Nature, 579(7799), 385–392, doi:10.1038/s41586-020-2084-4, 2020.

Ashok, K., Behera, S. K., Rao, S. A., Weng, H. and Yamagata, T.: El Niño Modoki and its possible teleconnection, J. Geophys. Res. Ocean., 112(11), 1–27, doi:10.1029/2006JC003798, 2007.

Bao, H., Niggemann, J., Luo, L., Dittmar, T. and Kao, S. J.: Aerosols as a source of dissolved black carbon to the ocean, Nat. Commun., 8(1), doi:10.1038/s41467-017-00437-3, 2017.

Boy, J. and Wilcke, W.: Tropical Andean forest derives calcium and magnesium from Saharan dust, Global Biogeochem. Cycles, 22(1), 1–11, doi:10.1029/2007GB002960, 2008.

Bullard, J. E., Baddock, M., Bradwell, T., Crusius, J., Darlington, E., Gaiero, D., Gassó, S., Gisladottir, G., Hodgkins, R., McCulloch, R., McKenna-Neuman, C., Mockford, T., Stewart, H. and Thorsteinsson, T.: High-latitude dust in the Earth system, Rev. Geophys., 54(2), 447–485, doi:10.1002/2016RG000518, 2016.

Cai, W., Sullivan, A. and Cowan, T.: Interactions of ENSO, the IOD, and the SAM in CMIP3 Models, J. Clim., 24(6), 1688–1704, doi:10.1175/2010JCLI3744.1, 2011.

Cai, W., Wu, L., Lengaigne, M., Li, T., McGregor, S., Kug, J.-S., Yu, J.-Y., Stuecker, M. F., Santoso, A., Li, X., Ham, Y.-G., Chikamoto, Y., Ng, B., McPhaden, M. J., Du, Y., Dommenget, D., Jia, F., Kajtar, J. B., Keenlyside, N., Lin, X., Luo, J.-J., Martín-Rey, M., Ruprich-Robert, Y., Wang, G., Xie, S.-P., Yang, Y., Kang, S. M., Choi, J.-Y., Gan, B., Kim, G.-I., Kim, C.-E., Kim, S., Kim, J.-H. and Chang, P.: Pantropical climate interactions, Science (80-.)., 363(6430), eaav4236, doi:10.1126/science.aav4236, 2019.

Cai, W., Santoso, A., Collins, M., Dewitte, B., Karamperidou, C., Kug, J.-S., Lengaigne, M., McPhaden, M. J., Stuecker, M. F., Taschetto, A. S., Timmermann, A., Wu, L., Yeh, S.-W., Wang, G., Ng, B., Jia, F., Yang, Y., Ying, J., Zheng, X.-T., Bayr, T., Brown, J. R., Capotondi, A., Cobb, K. M., Gan, B., Geng, T., Ham, Y.-G., Jin, F.-F., Jo, H.-S., Li, X., Lin, X., McGregor, S., Park, J.-H., Stein, K., Yang, K., Zhang, L. and Zhong, W.: Changing El Niño–Southern Oscillation in a warming climate, Nat. Rev. Earth Environ., 2(9), 628–644, doi:10.1038/s43017-021-00199-z, 2021.

Carslaw, K. S., Boucher, O., Spracklen, D. V., Mann, G. W., Rae, J. G. L., Woodward, S. and Kulmala, M.: A review of

natural aerosol interactions and feedbacks within the Earth system, Atmos. Chem. Phys., 10(4), 1701–1737, doi:10.5194/acp-10-1701-2010, 2010.

Collins, W. J., Lamarque, J.-F., Schulz, M., Boucher, O., Eyring, V., Hegglin, M. I., Maycock, A., Myhre, G., Prather, M., Shindell, D. and Smith, S. J.: AerChemMIP: quantifying the effects of chemistry and aerosols in CMIP6, Geosci. Model Dev., 10(2), 585–607, doi:10.5194/gmd-10-585-2017, 2017.

Creamean, J. M., Suski, K. J., Rosenfeld, D., Cazorla, A., DeMott, P. J., Sullivan, R. C., White, A. B., Ralph, F. M., Minnis, P., Comstock, J. M., Tomlinson, J. M. and Prather, K. A.: Dust and Biological Aerosols from the Sahara and Asia Influence Precipitation in the Western U.S., Science (80-.)., 339(6127), 1572–1578, doi:10.1126/science.1227279, 2013.

D'Odorico, P., Bhattachan, A., Davis, K. F., Ravi, S. and Runyan, C. W.: Global desertification: Drivers and feedbacks, Adv. Water Resour., 51, 326–344, doi:10.1016/j.advwatres.2012.01.013, 2013.

Dai, A. and Wigley, T. M. L.: Global patterns of ENSO-induced precipitation, Geophys. Res. Lett., 27(9), 1283–1286, doi:10.1029/1999GL011140, 2000.

Delworth, T. L., Zeng, F., Vecchi, G. A., Yang, X., Zhang, L. and Zhang, R.: The North Atlantic Oscillation as a driver of rapid climate change in the Northern Hemisphere, Nat. Geosci., 9(7), 509–512, doi:10.1038/ngeo2738, 2016.

van der Does, M., Brummer, G. J. A., van Crimpen, F. C. J., Korte, L. F., Mahowald, N. M., Merkel, U., Yu, H., Zuidema, P. and Stuut, J. B. W.: Tropical Rains Controlling Deposition of Saharan Dust Across the North Atlantic Ocean, Geophys. Res. Lett., 47(5), 1–10, doi:10.1029/2019GL086867, 2020.

Duan, X., Guo, C., Zhang, C., Li, H., Zhou, Y., Gao, H., Xia, X., He, H., McMinn, A. and Wang, M.: Effect of East Asian atmospheric particulate matter deposition on bacterial activity and community structure in the oligotrophic Northwest Pacific, Environ. Pollut., 283, 117088, doi:10.1016/j.envpol.2021.117088, 2021.

Duniway, M. C., Pfennigwerth, A. A., Fick, S. E., Nauman, T. W., Belnap, J. and Barger, N. N.: Wind erosion and dust from US drylands: a review of causes, consequences, and solutions in a changing world, Ecosphere, 10(3), doi:10.1002/ecs2.2650, 2019.

Evan, A. T., Foltz, G. R., Zhang, D. and Vimont, D. J.: Influence of African dust on ocean–atmosphere variability in the tropical Atlantic, Nat. Geosci., 4(11), 762–765, doi:10.1038/ngeo1276, 2011.

Eyring, V., Bony, S., Meehl, G. A., Senior, C. A., Stevens, B., Stouffer, R. J. and Taylor, K. E.: Overview of the Coupled Model Intercomparison Project Phase 6 (CMIP6) experimental design and organization, Geosci. Model Dev., 9(5), 1937–1958, doi:10.5194/gmd-9-1937-2016, 2016.

Fan, S. M., Moxim, W. J. and Levy, H.: Aeolian input of bioavailable iron to the ocean, Geophys. Res. Lett., 33(7), 2–5, doi:10.1029/2005GL024852, 2006.

Garfinkel, C. I., Hurwitz, M. M., Waugh, D. W. and Butler, A. H.: Are the teleconnections of Central Pacific and Eastern Pacific El Niño distinct in boreal wintertime?, Clim. Dyn., 41(7–8), 1835–1852, doi:10.1007/s00382-012-1570-2, 2013.

Guo, J., Lou, M., Miao, Y., Wang, Y., Zeng, Z., Liu, H., He, J., Xu, H., Wang, F., Min, M. and Zhai, P.: Trans-Pacific transport of dust aerosols from East Asia: Insights gained from multiple observations and modeling, Environ. Pollut., 230,

1030–1039, doi:10.1016/j.envpol.2017.07.062, 2017.

Huang, Y., Liu, X., Yin, Z. Y. and An, Z.: Global Impact of ENSO on Dust Activities with Emphasis on the Key Region from the Arabian Peninsula to Central Asia, J. Geophys. Res. Atmos., 126(9), 1–24, doi:10.1029/2020JD034068, 2021.

Hurrell, J. W., Kushnir, Y., Ottersen, G. and Visbeck, M.: An overview of the North Atlantic Oscillation, in Geophysical Monograph American Geophysical Union, pp. 1–35, American Geophysical Union., 2003.

Itahashi, S., Hayashi, K., Takeda, S., Umezawa, Y., Matsuda, K., Sakurai, T. and Uno, I.: Nitrogen burden from atmospheric deposition in East Asian oceans in 2010 based on high-resolution regional numerical modeling, Environ. Pollut., 286(April), 117309, doi:10.1016/j.envpol.2021.117309, 2021.

Jeong, J. I., Park, R. J. and Yeh, S. W.: Dissimilar effects of two El Niño types on PM2.5 concentrations in East Asia, Environ. Pollut., 242, 1395–1403, doi:10.1016/j.envpol.2018.08.031, 2018.

Jickells, T. D., An, Z. S., Andersen, K. K., Baker, A. R., Bergametti, C., Brooks, N., Cao, J. J., Boyd, P. W., Duce, R. A., Hunter, K. A., Kawahata, H., Kubilay, N., LaRoche, J., Liss, P. S., Mahowald, N., Prospero, J. M., Ridgwell, A. J., Tegen, I. and Torres, R.: Global iron connections between desert dust, ocean biogeochemistry, and climate, Science (80-.)., 308(5718), 67–71, doi:10.1126/science.1105959, 2005.

Jiménez, L., Rühland, K. M., Jeziorski, A., Smol, J. P. and Pérez-Martínez, C.: Climate change and Saharan dust drive recent cladoceran and primary production changes in remote alpine lakes of Sierra Nevada, Spain, Glob. Chang. Biol., 24(1), e139–e158, doi:10.1111/gcb.13878, 2018.

Kanakidou, M., Myriokefalitakis, S. and Tsigaridis, K.: Aerosols in atmospheric chemistry and biogeochemical cycles of nutrients, Environ. Res. Lett., 13(6), doi:10.1088/1748-9326/aabcdb, 2018.

Knippertz, P. and Todd, M. C.: Mineral dust aerosols over the Sahara: Meteorological controls on emission and transport and implications for modeling, Rev. Geophys., 50(1), doi:10.1029/2011RG000362, 2012.

Kohfeld, K. E., Le Quéré, C., Harrison, S. P. and Anderson, R. F.: Role of marine biology in glacial-interglacial CO2 cycles, Science (80-.)., 308(5718), 74–78, doi:10.1126/science.1105375, 2005.

Kok, J. F., Ward, D. S., Mahowald, N. M. and Evan, A. T.: Global and regional importance of the direct dust-climate feedback, Nat. Commun., 9(1), doi:10.1038/s41467-017-02620-y, 2018.

Kok, J. F., Adebiyi, A. A., Albani, S., Balkanski, Y., Checa-Garcia, R., Chin, M., Colarco, P. R., Hamilton, D. S., Huang, Y., Ito, A., Klose, M., Leung, D. M., Li, L., Mahowald, N. M., Miller, R. L., Obiso, V., Pérez García-Pando, C., Rocha-Lima, A., Wan, J. S. and Whicker, C. A.: Improved representation of the global dust cycle using observational constraints on dust properties and abundance, Atmos. Chem. Phys., 21(10), 8127–8167, doi:10.5194/acp-21-8127-2021, 2021.

Kripalani, R. H. and Kulkarni, A.: Rainfall variability over South-East Asia - Connections with Indian monsoon and Enso extremes: New perspectives, Int. J. Climatol., 17(11), 1155–1168, doi:10.1002/(SICI)1097-0088(199709)17:11<1155::AID-JOC188>3.0.CO;2-B, 1997.

Kripalani, R. H., Oh, J. H. and Chaudhari, H. S.: Delayed influence of the Indian Ocean Dipole mode on the East Asia-West Pacific monsoon: possible mechanism, Int. J. Climatol., 30(2), 197–209, doi:10.1002/joc.1890, 2009.

Le, T. and Bae, D.-H.: Response of global evaporation to major climate modes in historical and future Coupled Model Intercomparison Project Phase 5 simulations, Hydrol. Earth Syst. Sci., 24(3), 1131–1143, doi:10.5194/hess-24-1131-2020, 2020.

Le, T. and Bae, D.-H. H.: Causal links on interannual timescale between ENSO and the IOD in CMIP5 future simulations, Geophys. Res. Lett., 46(5), 1–9, doi:10.1029/2018GL081633, 2019.

Le, T., Ha, K.-J. J., Bae, D.-H. H. and Kim, S.-H. H.: Causal effects of Indian Ocean Dipole on El Niño-Southern Oscillation during 1950-2014 based on high-resolution models and reanalysis data, Environ. Res. Lett., 15(10), 1040b6, doi:10.1088/1748-9326/abb96d, 2020.

Le, T., Ha, K.-J. and Bae, D.-H.: Projected response of global runoff to El Niño-Southern oscillation, Environ. Res. Lett., 16(8), 084037, doi:10.1088/1748-9326/ac13ed, 2021.

Le, T., Kim, S. and Bae, D.: Decreasing causal impacts of El Niño–Southern Oscillation on future fire activities, Sci. Total Environ., 826, 154031, doi:10.1016/j.scitotenv.2022.154031, 2022.

Li, Y., Mickley, L. J. and Kaplan, J. O.: Response of dust emissions in southwestern North America to 21st century trends in climate, CO₂ fertilization, and land use: implications for air quality, Atmos. Chem. Phys., 21(1), 57–68, doi:10.5194/acp-21-57-2021, 2021.

Li, Z., Wang, Y., Guo, J., Zhao, C., Cribb, M. C., Dong, X., Fan, J., Gong, D., Huang, J., Jiang, M., Jiang, Y., Lee, S. S., Li, H., Li, J., Liu, J., Qian, Y., Rosenfeld, D., Shan, S., Sun, Y., Wang, H., Xin, J., Yan, X., Yang, X., Yang, X. qun, Zhang, F. and Zheng, Y.: East Asian Study of Tropospheric Aerosols and their Impact on Regional Clouds, Precipitation, and Climate (EAST-AIRCPC), J. Geophys. Res. Atmos., 124(23), 13026–13054, doi:10.1029/2019JD030758, 2019.

de Longueville, F., Ozer, P., Doumbia, S. and Henry, S.: Desert dust impacts on human health: an alarming worldwide reality and a need for studies in West Africa, Int. J. Biometeorol., 57(1), 1–19, doi:10.1007/s00484-012-0541-y, 2013.

Luo, J.-J., Sasaki, W. and Masumoto, Y.: Indian Ocean warming modulates Pacific climate change, Proc. Natl. Acad. Sci., 109(46), 18701–18706, doi:10.1073/pnas.1210239109, 2012.

Marx, S. K., McGowan, H. A. and Kamber, B. S.: Long-range dust transport from eastern Australia: A proxy for Holocene aridity and ENSO-type climate variability, Earth Planet. Sci. Lett., 282(1–4), 167–177, doi:10.1016/j.epsl.2009.03.013, 2009.

Mosedale, T. J., Stephenson, D. B., Collins, M. and Mills, T. C.: Granger Causality of Coupled Climate Processes: Ocean Feedback on the North Atlantic Oscillation, J. Clim., 19(7), 1182–1194, doi:10.1175/JCLI3653.1, 2006.

Moulin, C. and Chiapello, I.: Impact of human-induced desertification on the intensification of Sahel dust emission and export over the last decades, Geophys. Res. Lett., 33(18), 1–5, doi:10.1029/2006GL025923, 2006.

Mulcahy, J. P., Johnson, C., Jones, C. G., Povey, A. C., Scott, C. E., Sellar, A., Turnock, S. T., Woodhouse, M. T., Abraham, N. L., Andrews, M. B., Bellouin, N., Browse, J., Carslaw, K. S., Dalvi, M., Folberth, G. A., Glover, M., Grosvenor, D. P., Hardacre, C., Hill, R., Johnson, B., Jones, A., Kipling, Z., Mann, G., Mollard, J., O'Connor, F. M., Palmiéri, J., Reddington, C., Rumbold, S. T., Richardson, M., Schutgens, N. A. J., Stier, P., Stringer, M., Tang, Y., Walton, J., Woodward, S. and

Yool, A.: Description and evaluation of aerosol in UKESM1 and HadGEM3-GC3.1 CMIP6 historical simulations, Geosci. Model Dev., 13(12), 6383–6423, doi:10.5194/gmd-13-6383-2020, 2020.

Perry, K. D., Cahill, T. A., Eldred, R. A., Dutcher, D. D. and Gill, T. E.: Long-range transport of North African dust to the eastern United States, J. Geophys. Res. Atmos., 102(D10), 11225–11238, doi:10.1029/97JD00260, 1997.

Pi, H., Sharratt, B. and Lei, J.: Wind erosion and dust emissions in central Asia: Spatiotemporal simulations in a typical dust year, Earth Surf. Process. Landforms, 44(2), 521–534, doi:10.1002/esp.4514, 2019.

Prospero, J. M. and Mayol-Bracero, O. L.: Understanding the transport and impact of African dust on the Caribbean Basin, Bull. Am. Meteorol. Soc., 94(9), 1329–1337, doi:10.1175/BAMS-D-12-00142.1, 2013.

Rap, A., Scott, C. E., Reddington, C. L., Mercado, L., Ellis, R. J., Garraway, S., Evans, M. J., Beerling, D. J., MacKenzie, A. R., Hewitt, C. N. and Spracklen, D. V.: Enhanced global primary production by biogenic aerosol via diffuse radiation fertilization, Nat. Geosci., 11(9), 640–644, doi:10.1038/s41561-018-0208-3, 2018.

Raphael, M. N. and Holland, M. M.: Twentieth century simulation of the southern hemisphere climate in coupled models. Part 1: Large scale circulation variability, Clim. Dyn., 26(2–3), 217–228, doi:10.1007/s00382-005-0082-8, 2006.

Rotstayn, L. D., Collier, M. A., Mitchell, R. M., Qin, Y., Campbell, S. K. and Dravitzki, S. M.: Simulated enhancement of ENSO-related rainfall variability due to Australian dust, Atmos. Chem. Phys., 11(13), 6575–6592, doi:10.5194/acp-11-6575-2011, 2011.

Roxy, M. K., Ritika, K., Terray, P., Murtugudde, R., Ashok, K. and Goswami, B. N.: Drying of Indian subcontinent by rapid Indian ocean warming and a weakening land-sea thermal gradient, Nat. Commun., 6(May), 7423, doi:10.1038/ncomms8423, 2015.

Saji, N. H., Goswami, B. N., Vinayachandran, P. N. and Yamagata, T.: A dipole mode in the tropical Indian Ocean, Nature, 401(6751), 360–363, doi:10.1038/43854, 1999.

Schulz, M., Prospero, J. M., Baker, A. R., Dentener, F., Ickes, L., Liss, P. S., Mahowald, N. M., Nickovic, S., García-Pando, C. P., Rodríguez, S., Sarin, M., Tegen, I. and Duce, R. A.: Atmospheric transport and deposition of mineral dust to the ocean: Implications for research needs, Environ. Sci. Technol., 46(19), 10390–10404, doi:10.1021/es300073u, 2012.

Schwarz, G.: Estimating the dimension of a model, Ann. Stat. [online] Available from: http://projecteuclid.org/euclid.aos/1176344136 (Accessed 30 May 2014), 1978.

Scott, C. E., Arnold, S. R., Monks, S. A., Asmi, A., Paasonen, P. and Spracklen, D. V.: Substantial large-scale feedbacks between natural aerosols and climate, Nat. Geosci., 11(1), 44–48, doi:10.1038/s41561-017-0020-5, 2018.

Shahsavani, A., Tobías, A., Querol, X., Stafoggia, M., Abdolshahnejad, M., Mayvaneh, F., Guo, Y., Hadei, M., Saeed Hashemi, S., Khosravi, A., Namvar, Z., Yarahmadi, M. and Emam, B.: Short-term effects of particulate matter during desert and non-desert dust days on mortality in Iran, Environ. Int., 134(October 2019), 105299, doi:10.1016/j.envint.2019.105299, 2020.

Shao, Y., Klose, M. and Wyrwoll, K.-H.: Recent global dust trend and connections to climate forcing, J. Geophys. Res. Atmos., 118(19), 11,107-11,118, doi:10.1002/jgrd.50836, 2013.

Stern, D. I. and Kaufmann, R. K.: Anthropogenic and natural causes of climate change, Clim. Change, 122(1–2), 257–269, doi:10.1007/s10584-013-1007-x, 2013.

Tagliabue, A., Bopp, L., Dutay, J. C., Bowie, A. R., Chever, F., Jean-Baptiste, P., Bucciarelli, E., Lannuzel, D., Remenyi, T., Sarthou, G., Aumont, O., Gehlen, M. and Jeandel, C.: Hydrothermal contribution to the oceanic dissolved iron inventory, Nat. Geosci., 3(4), 252–256, doi:10.1038/ngeo818, 2010.

Taschetto, A. S. and England, M. H.: El Niño Modoki impacts on Australian rainfall, J. Clim., 22(11), 3167–3174, doi:10.1175/2008JCLI2589.1, 2009.

Thornhill, G., Collins, W., Olivié, D., Archibald, A., Bauer, S., Checa-Garcia, R., Fiedler, S., Folberth, G., Gjermundsen, A., Horowitz, L., Lamarque, J.-F., Michou, M., Mulcahy, J., Nabat, P., Naik, V., O'Connor, F., Paulot, F., Schulz, M., Scott, C., Seferian, R., Smith, C., Takemura, T., Tilmes, S. and Weber, J.: Climate-driven chemistry and aerosol feedbacks in CMIP6 Earth system models, Atmos. Chem. Phys., 1–36, doi:10.5194/acp-2019-1207, 2020.

Timmermann, A., An, S. Il, Kug, J. S., Jin, F. F., Cai, W., Capotondi, A., Cobb, K., Lengaigne, M., McPhaden, M. J., Stuecker, M. F., Stein, K., Wittenberg, A. T., Yun, K. S., Bayr, T., Chen, H. C., Chikamoto, Y., Dewitte, B., Dommenget, D., Grothe, P., Guilyardi, E., Ham, Y. G., Hayashi, M., Ineson, S., Kang, D., Kim, S., Kim, W. M., Lee, J. Y., Li, T., Luo, J. J., McGregor, S., Planton, Y., Power, S., Rashid, H., Ren, H. L., Santoso, A., Takahashi, K., Todd, A., Wang, G., Wang, G., Xie, R., Yang, W. H., Yeh, S. W., Yoon, J., Zeller, E. and Zhang, X.: El Niño–Southern Oscillation complexity, Nature, 559(7715), 535–545, doi:10.1038/s41586-018-0252-6, 2018.

Tong, D. Q., Wang, J. X. L., Gill, T. E., Lei, H. and Wang, B.: Intensified dust storm activity and Valley fever infection in the southwestern United States, Geophys. Res. Lett., 44(9), 4304–4312, doi:10.1002/2017GL073524, 2017.

Ummenhofer, C. C., England, M. H., McIntosh, P. C., Meyers, G. A., Pook, M. J., Risbey, J. S., Sen Gupta, A. and Taschetto, A. S.: What causes southeast Australia's worst droughts?, Geophys. Res. Lett., 36(4), L04706, doi:10.1029/2008GL036801, 2009.

Webb, N. P. and Pierre, C.: Quantifying Anthropogenic Dust Emissions, Earth's Futur., 6(2), 286–295, doi:10.1002/2017EF000766, 2018.

Webster, P. J., Moore, A. M., Loschnigg, J. P. and Leben, R. R.: Coupled ocean–atmosphere dynamics in the Indian Ocean during 1997–98, Nature, 401(6751), 356–360, doi:10.1038/43848, 1999.

Xu, H., Guo, J., Wang, Y., Zhao, C., Zhang, Z., Min, M., Miao, Y., Liu, H., He, J., Zhou, S. and Zhai, P.: Warming effect of dust aerosols modulated by overlapping clouds below, Atmos. Environ., 166, 393–402, doi:10.1016/j.atmosenv.2017.07.036, 2017.

Yang, Y., Russell, L. M., Lou, S., Liao, H., Guo, J., Liu, Y., Singh, B. and Ghan, S. J.: Dust-wind interactions can intensify aerosol pollution over eastern China, Nat. Commun., 8(May), 1–8, doi:10.1038/ncomms15333, 2017.

Yeh, S. W., Cai, W., Min, S. K., McPhaden, M. J., Dommenget, D., Dewitte, B., Collins, M., Ashok, K., An, S. Il, Yim, B. Y. and Kug, J. S.: ENSO Atmospheric Teleconnections and Their Response to Greenhouse Gas Forcing, Rev. Geophys., 56(1), 185–206, doi:10.1002/2017RG000568, 2018.

Yu, J. Y. and Zou, Y.: The enhanced drying effect of Central-Pacific El Niño on US winter, Environ. Res. Lett., 8(1), doi:10.1088/1748-9326/8/1/014019, 2013.

Zhang, X.-X., Sharratt, B., Liu, L.-Y., Wang, Z.-F., Pan, X.-L., Lei, J.-Q., Wu, S.-X., Huang, S.-Y., Guo, Y.-H., Li, J., Tang, X., Yang, T., Tian, Y., Chen, X.-S., Hao, J.-Q., Zheng, H.-T., Yang, Y.-Y. and Lyu, Y.-L.: East Asian dust storm in May 2017: observations, modelling, and its influence on the Asia-Pacific region, Atmos. Chem. Phys., 18(11), 8353–8371, doi:10.5194/acp-18-8353-2018, 2018.

Zhao, A., Ryder, C. L. and Wilcox, L. J.: How well do the CMIP6 models simulate dust aerosols?, Atmos. Chem. Phys., 22(3), 2095–2119, doi:10.5194/acp-22-2095-2022, 2022.

MODELS MEAN: ENSO - DRY DUST PERIOD 1850-2014 EXPERIMENT HISTORICAL

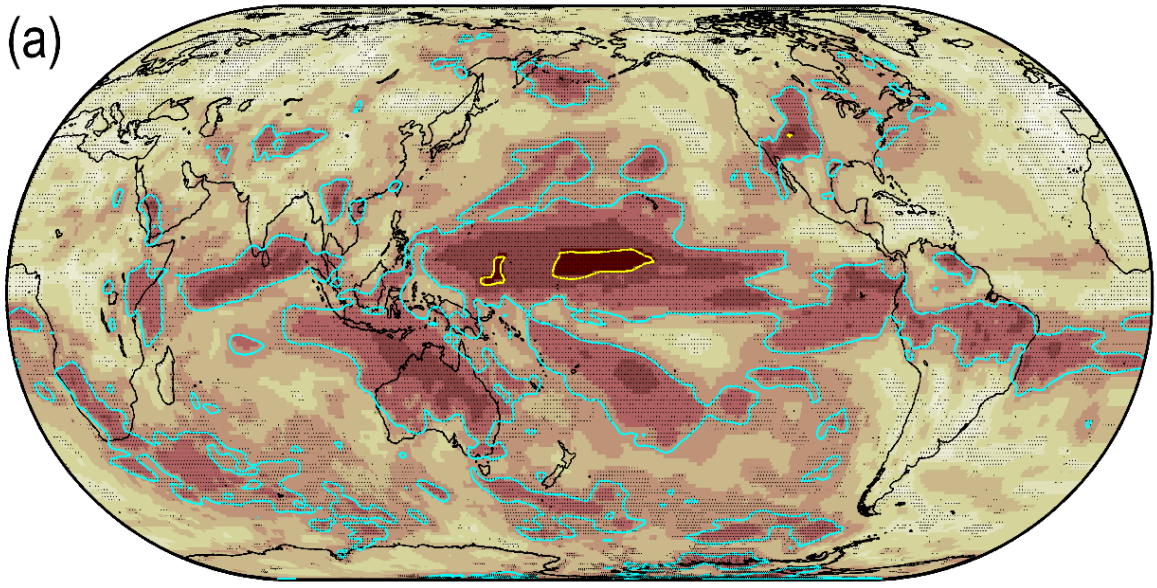

MODELS MEAN: ENSO - WET DUST PERIOD 1850-2014 EXPERIMENT HISTORICAL

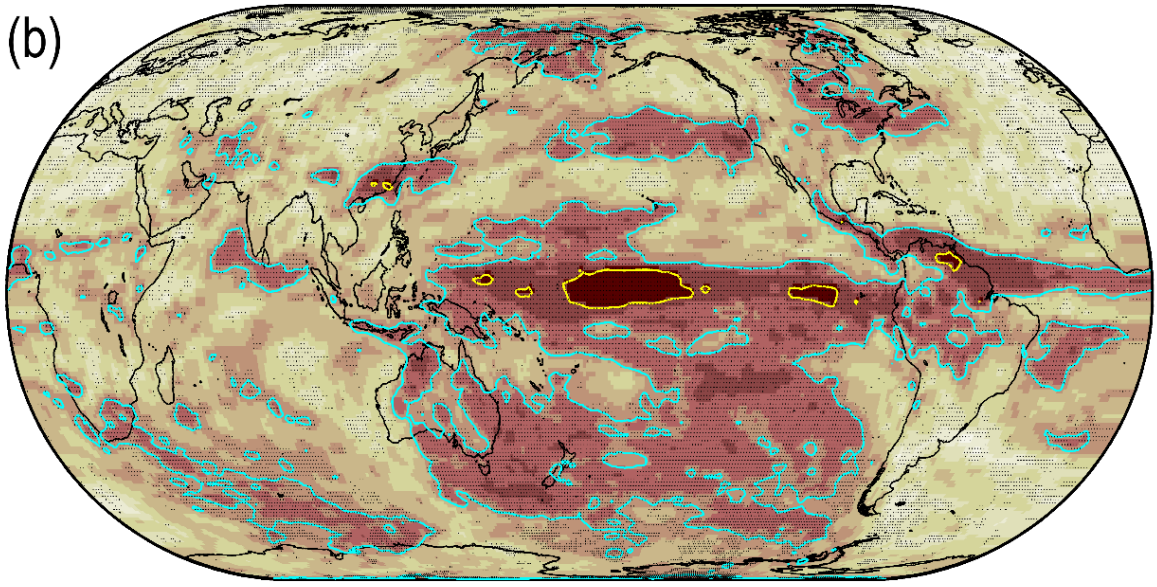

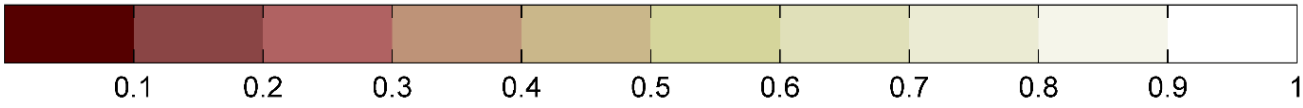

Figure 1. Multi-model mean probability map for the absence of Granger causality from ENSO to annual mean deposition rate of dry dust (a) and wet dust (b) over the period 1850-2014 of the historical experiment. Stippling indicates that no less than 70% of all models show agreement on the mean probability of total models at a given grid point. The agreement of an individual model is specified when the difference between the multi-model mean probability and the selected model's probability is less than one standard deviation of the multi-model mean probability. The cyan and yellow contour lines specify *p*-value = 0.33 and 0.1, respectively. Brown shades imply a low probability for no Granger causality. ENSO: El Niño–Southern Oscillation.

MODELS MEAN: ENSO - OPTICAL DEPTH PERIOD 1850-2014 EXPERIMENT HISTORICAL

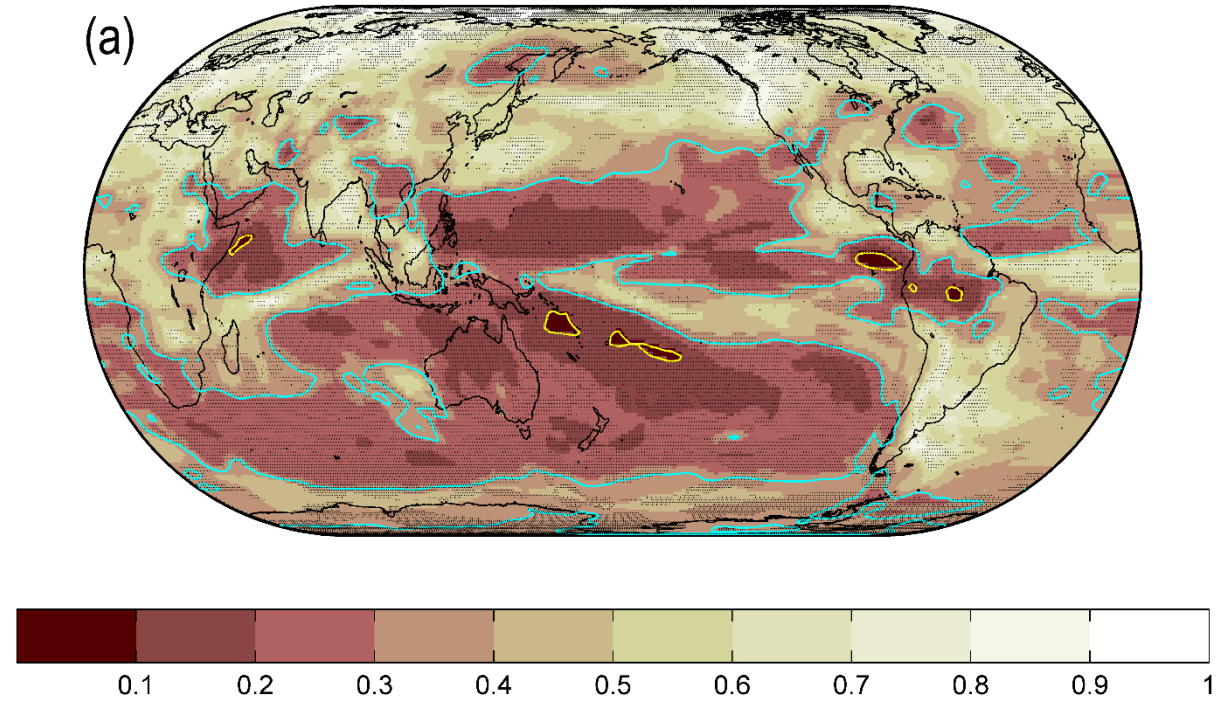

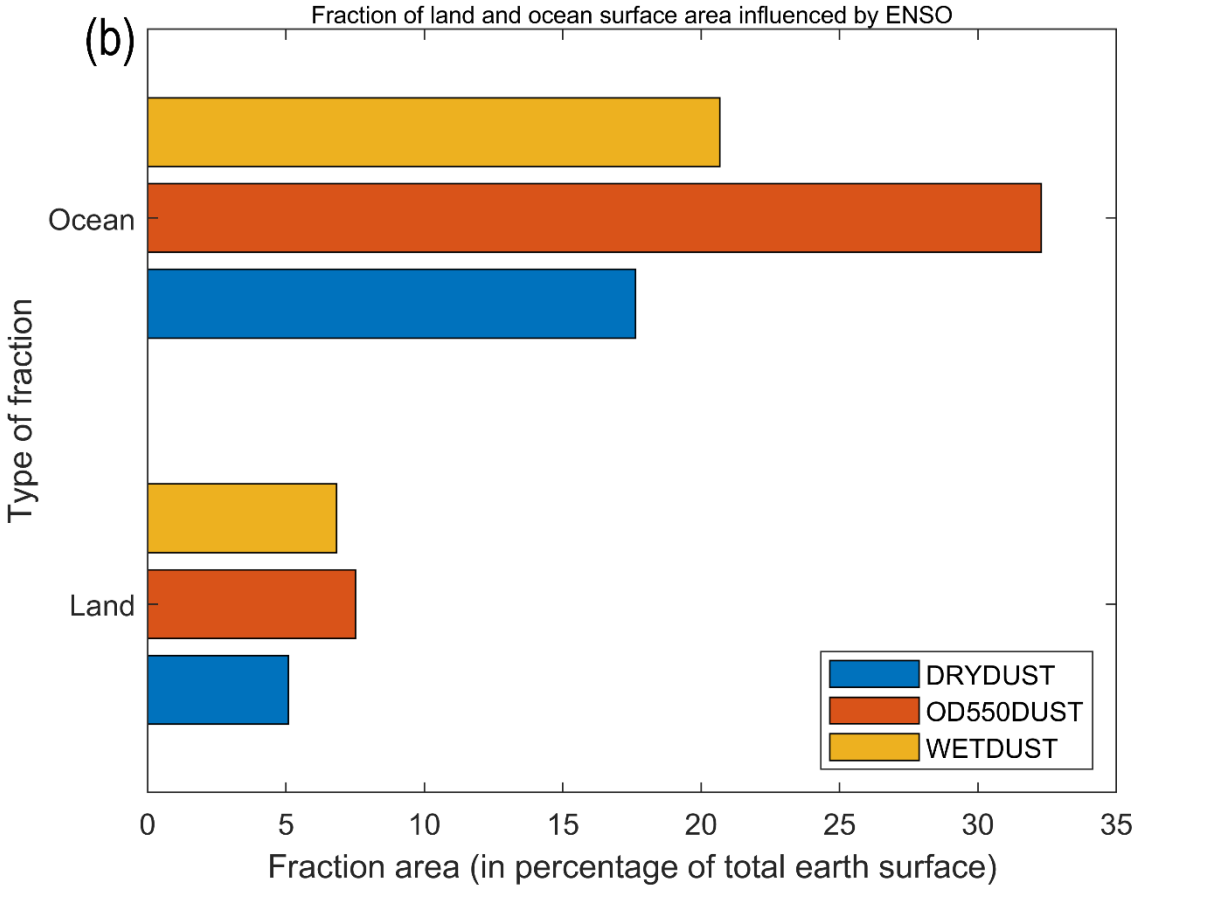

Figure 2. (a) As in Fig. 1, except for the probability for the absence of Granger causality from ENSO to annual mean dust aerosol optical depth over the period 1850-2014 for the historical experiment. (b) Fraction of total Earth-surface over land and ocean with probability for no Granger causality from ENSO to dust deposition and dust aerosol optical depth smaller than 0.33 (i.e., p-value < 0.33). Fraction areas affected by ENSO on dry dust, dust aerosol optical depth and wet dust are displayed in blue, red, and yellow bars, respectively. ENSO: El Niño–Southern Oscillation.

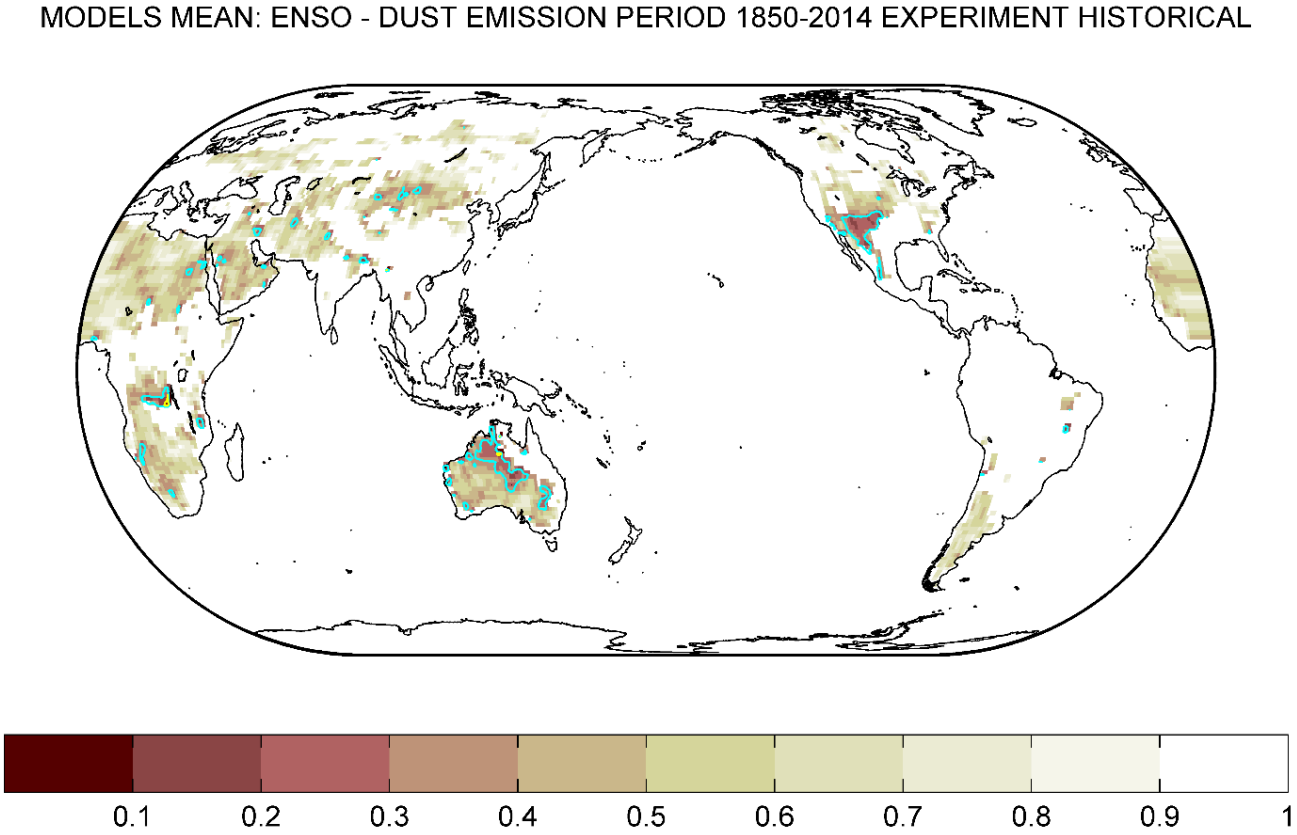

435

Figure 3. As in Fig. 1, except for the probability for the absence of Granger causality from ENSO to annual mean dust emission over the period 1850-2014 for the historical experiment. ENSO: El Niño–Southern Oscillation.

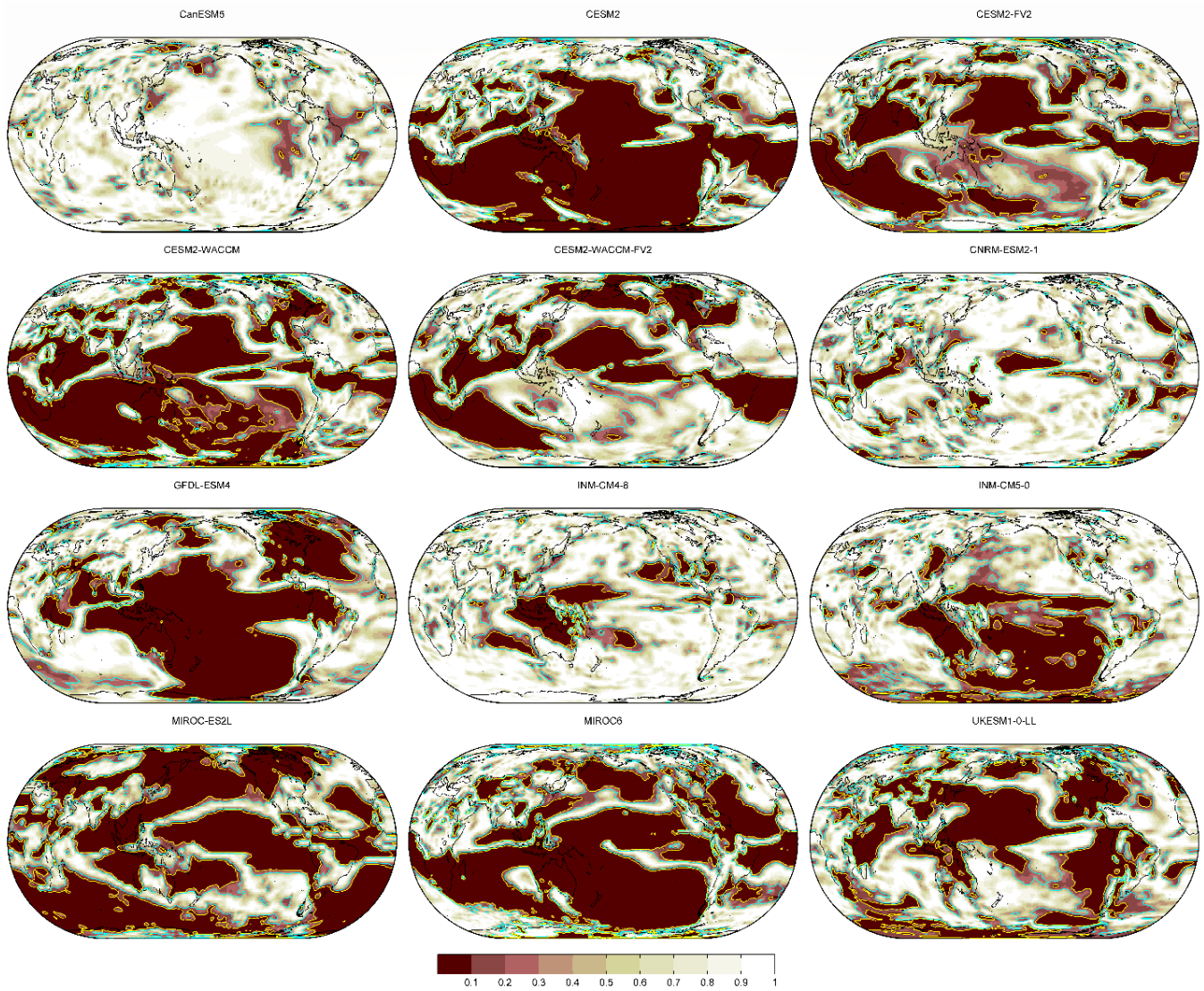

Figure 4. As in Fig. 1, except for the probability for the absence of Granger causality from ENSO to annual mean dry dust deposition over the period 1850-2014 for the historical simulation of 12 different models (see Tables S1 and S2). ENSO: El Niño–Southern Oscillation.

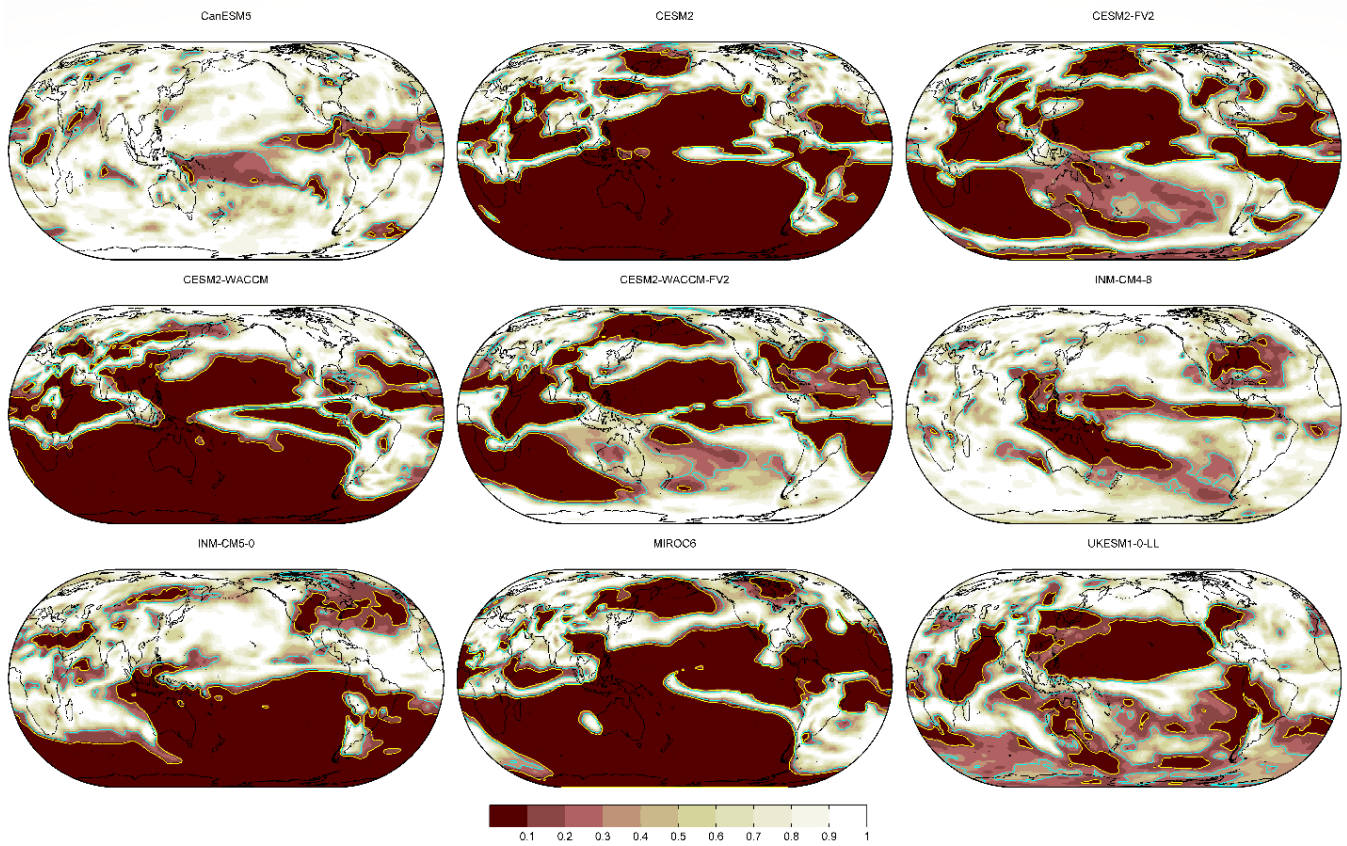

Figure 5. As in Fig. 1, except for the probability for the absence of Granger causality from ENSO to annual mean dust aerosol optical depth over the period 1850-2014 for the historical simulation of 9 different models (see Table S2). ENSO: El Niño–Southern Oscillation.

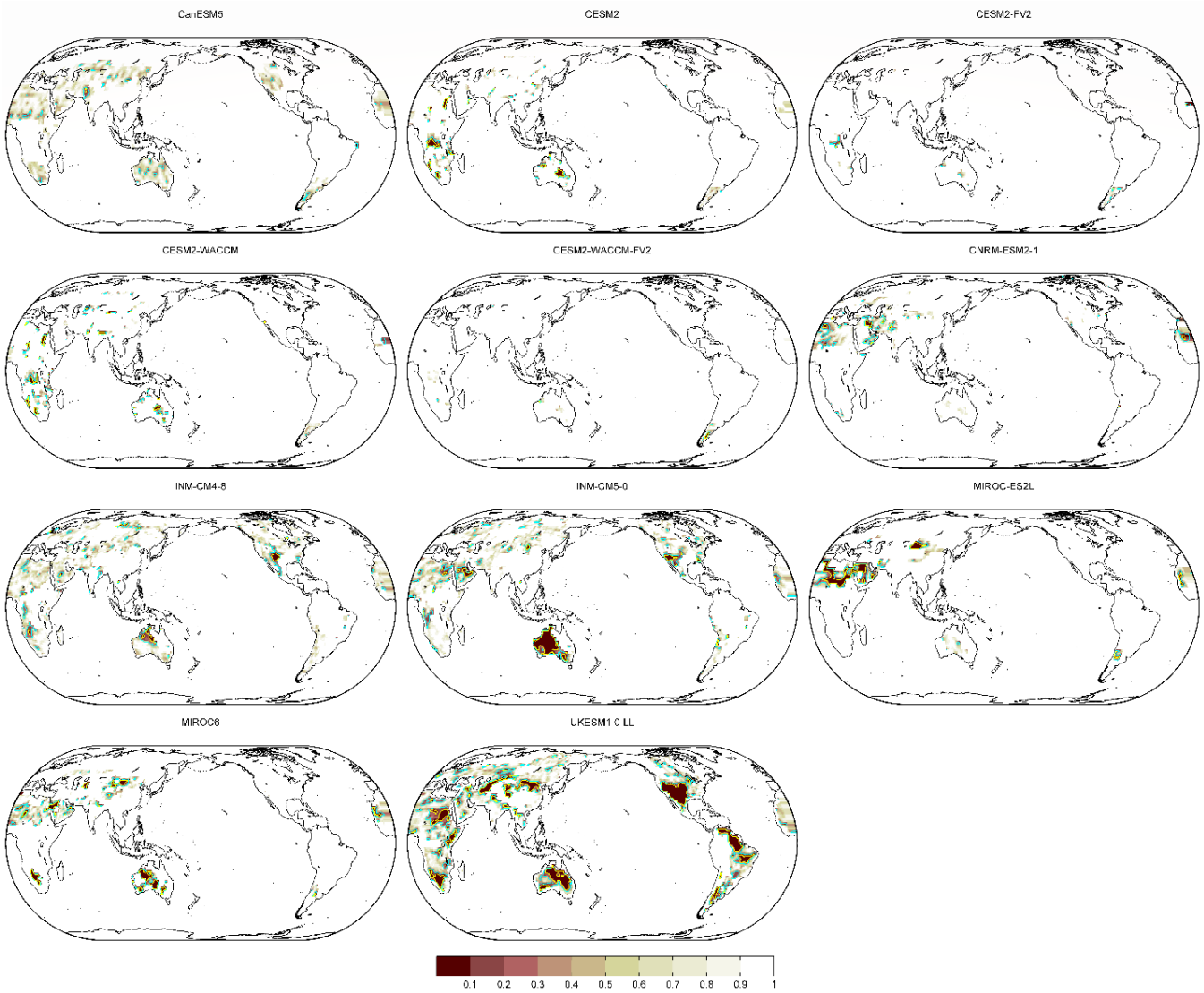

Figure 6. As in Fig. 1, except for the probability for the absence of Granger causality from ENSO to annual mean dust emission over the period 1850-2014 for the historical simulation of 11 different models (see Table S2). ENSO: El Niño–Southern Oscillation.